

# AWG OPTICAL DEMULTIPLEXERS: FROM DESIGN TO CHIP

*D. Seyringer*

*Research Centre for Microtechnology, Vorarlberg University of Applied Sciences,  
Hochschulstr. 1, 6850 Dornbirn, Austria,  
E-mail: dana.seyringer@fhv.at*

*Received 29 April 2013; accepted 03 May 2013*

## 1. Introduction

Wavelength division multiplexing (WDM) is the uncontested candidate for increasing capacity throughput of optical networks. Arrayed waveguide gratings (AWGs) are the most promising devices for filters or multi/demultiplexers in such WDM systems because of their low insertion loss, high stability, and low cost [1]. In recent years they become increasingly popular also for dense WDM (DWDM) applications. This popularity is largely due to the fact that AWGs have been proven capable of precisely demultiplexing a high number of optical signals (carrying information at various wavelengths) with relative low loss. They can be also included in a more complex management system, such as optical add drop multiplexers (OADMs) or variable optical amplifiers (VOAs).

## 2. AWG Functionality

The AWG consists of input/output waveguides, two couplers and an array of waveguides (also called phased array) with constant path-length difference  $dL$  as shown in Fig. 1. One of the input waveguides carries an optical signal consisting of multiple wavelengths,  $\lambda_1 - \lambda_n$ . The input coupler distributes the light among the array of waveguides. Then the light propagates through the waveguides to the output coupler. The length of arrayed waveguides is chosen so that the optical path-length difference between adjacent waveguides,  $dL$  equals an integer multiple of AWG central wavelength  $\lambda_c$  of the demultiplexer. For this wavelength the fields in the individual arrayed waveguides will arrive at the input of the output coupler with equal phase (apart from an integer multiple of  $2\pi$ ), and the field distribution at the output of the input coupler will be reproduced at the input of the output coupler. Linearly increasing length of arrayed waveguides will cause interference and diffraction when light mixes in the output coupler. As a result, each of the wavelengths  $\lambda_1 - \lambda_n$  is focused into only one of the  $N$  output waveguides [2].

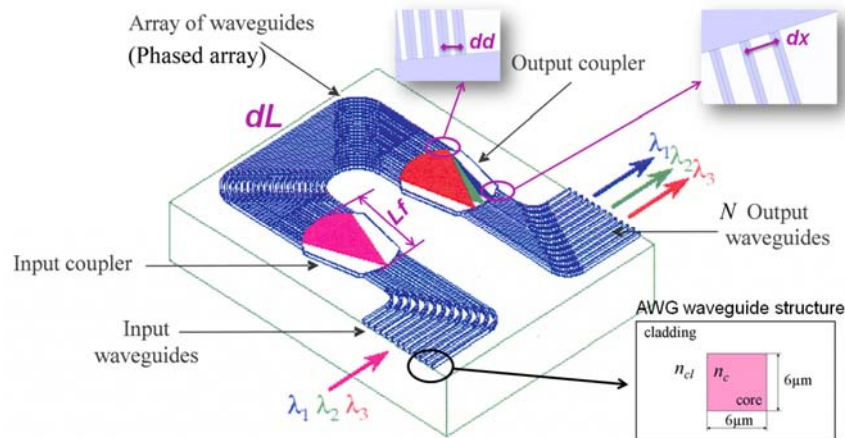


Fig.1: Principle of AWG with used AWG waveguide structure.

### 3. AWG design and simulation

When designing AWGs three different sets of input parameters have to be considered:

1) Technological parameters: refractive indices of the core,  $n_c$  and cladding,  $n_{cl}$  and the core size of the used waveguides. These parameters create an input for the design of AWG waveguide structure shown in Fig. 1.

2) AWG type parameters address the type of AWG that is going to be designed. These parameters are: the number of output waveguides - channels ( $N = 4, 8, 16\dots$ ), channel spacing ( $df = 100 \text{ GHz}, 50 \text{ GHz}, \text{etc.}$ ) and AWG centre wavelength,  $\lambda_c$ .

3) Transmission parameters: any AWG is designed to reach some transmission parameters like insertion loss uniformity over all the output channels (also called non-uniformity),  $Lu$ , adjacent channel crosstalk,  $Cr$ , insertion loss,  $IL$ , etc. These parameters define the performance of AWG and also determine its suitability for a particular application.

From above mentioned input design parameters the AWG geometrical parameters like: coupler length,  $L_f$ , minimum waveguide separation at the input/output,  $dx$ , minimum waveguide separation in phased array,  $dd$  and the length increment,  $dL$  (see Fig. 1) have to be calculated. They are the input for AWG layout that will be then created and simulated using commercial AWG design tools like Optiwave or Apollo Photonics. For this calculation we developed stand-alone AWG-Parameters software tool (for more information see [3]).

As an example we designed low-contrast refractive index 8-channel, 100 GHz AWG with a typical refractive index contrast of 0.75 %, where  $n_{cl} (n_{out}) = 1.445$  and  $n_c (n_{eff}) = 1.456$  (see Fig. 2-left “Material” window). The cross section of waveguide structure was set to  $6 \mu\text{m} \times 6 \mu\text{m}$  to ensure the single mode propagation only. The optical demultiplexer was designed for the AWG central wavelength  $\lambda_c$  ( $Lambda$ ) =  $1.55012 \mu\text{m}$  (see Fig. 2-left “Transmission parameters – AWG parameters” window). The theoretical transmission parameters that AWG was designed for were: insertion loss uniformity,  $Lu = 0.7 \text{ dB}$  and adjacent channel crosstalk,  $Cr = -30 \text{ dB}$  (Fig. 2-left “Transmission parameters – AWG parameters” window). The calculated geometrical parameters were:  $dx = 19.35 \mu\text{m}$ ,  $dd = 11.73 \mu\text{m}$ , coupler length  $L_f = 3010.136 \mu\text{m}$ , length increment in the phased array  $dL = 145.974 \mu\text{m}$  (see Fig. 2-left “Transmission parameters – AWG parameters” window). Based on these parameters the AWG layout was created using Optiwave and Apollo tools (see Fig. 2-right) and simulated.

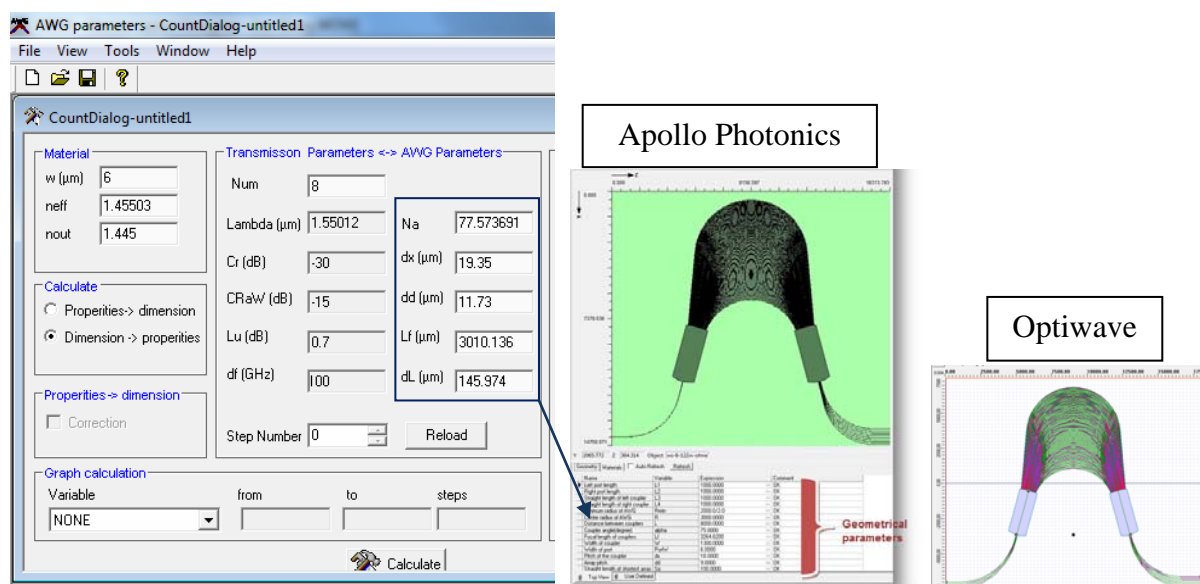


Fig. 2: User interface of AWG-Parameters tool (left) and AWG layouts created by Apollo Photonics and Optiwave tools (right).

#### 4. AWG Evaluation

The output of the simulation is an AWG spectral response, so called AWG transmission characteristics for TE and TM polarization (shown in Fig. 3-left). They create the basis for the calculation of AWG transmission parameters described in section 3, point 3). These parameters were calculated using our in-house developed software tool AWG-Analyzer (for more information see [4]) shown in Fig. 3-right. This tool calculates 18 transmission parameters (where  $ILu$  is  $Lu$ ,  $AX$  is  $Cr$ ,  $Ch$ . Spacing is  $df$  in AWG-Parameters tool).

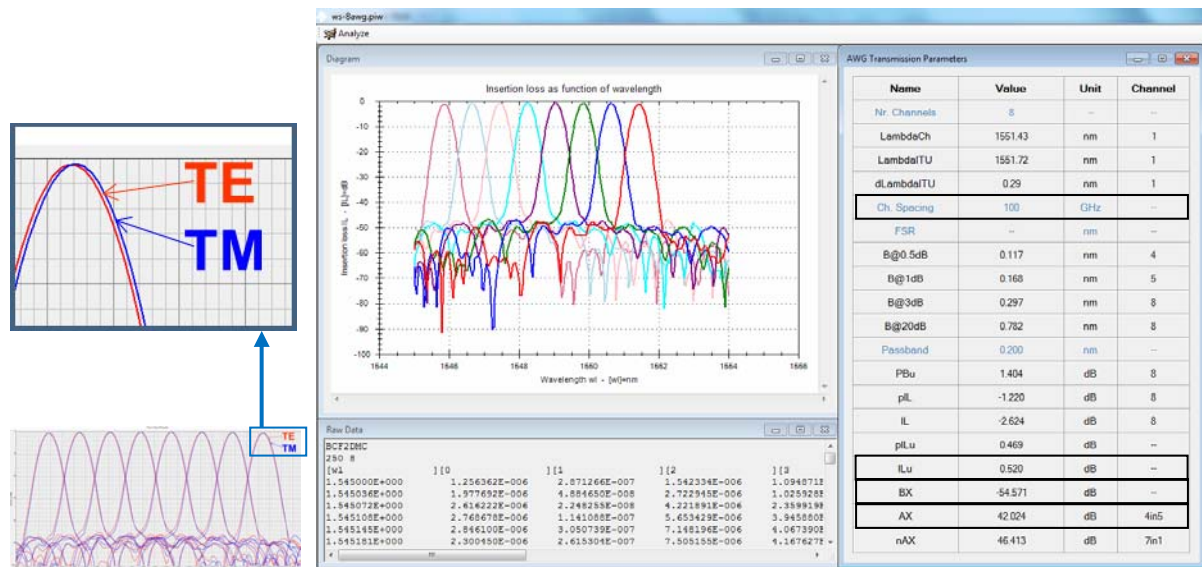


Fig. 3: AWG transmission characteristics from Optiwave tool (left) and user interface of AWG-Analyzer tool (right).

#### 5. AWG Fabrication

When AWG designs are finished and ready for the fabrication the next step is to export these designs usually in GDSII format. From all single GDSII files the whole mask layout will be generated and sent to a mask house for the production (Fig. 4-left). Produced mask will be later used in the lithography process to transfer the AWG structures onto the wafer.

From technological point of view, the AWG is a planar waveguide structure usually obtained on silicon wafer with a  $\text{SiO}_2$  lower cladding oxide obtained using thermal oxidation of Si substrate (having refractive index  $n_{cl}$ ). Chemical vapor deposition (CVD) process creates  $\text{GeSiO}_2$  active layer (so called “core”) with refractive index  $n_c$  higher than the refractive index of the cladding layer. Optical lithography and dry etching define then the AWG waveguide structure (shown in Fig. 1). The growth of upper cladding (CVD process) with refractive index matching with lower cladding is the last fabrication step (Fig. 5).

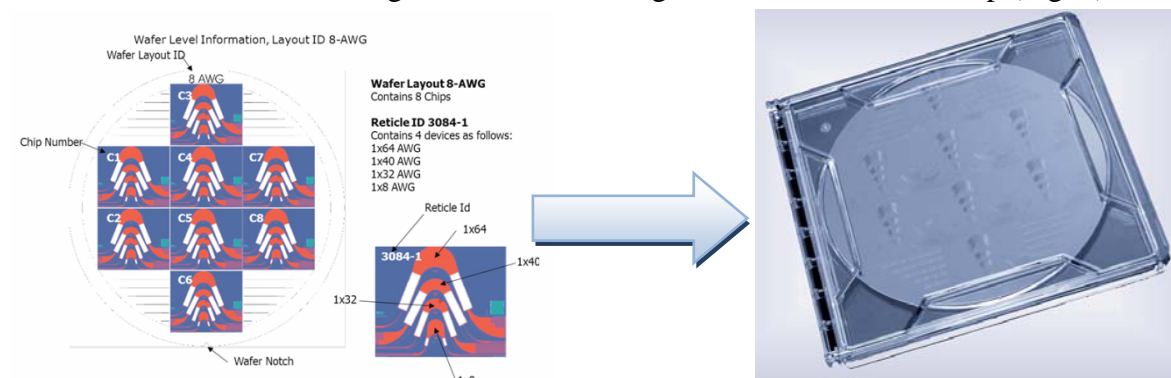


Fig. 4: Mask layout consisting of all AWG designs (left) and fabricated wafer (right).

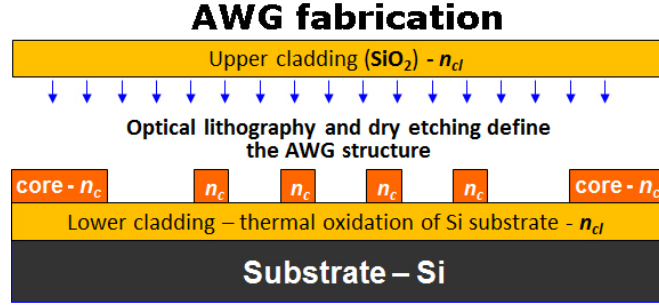


Fig. 5: AWG fabrication steps.

## 6. AWG Measurement

The fabricated chips have to be first diced and then can be measured on a wafer level (see Fig. 6). The measurement method adhered to by most AWG vendors is the deployment of the so called Mueller Matrix method. For this purpose the polarization controller is used to set the known polarization state at the input before the light enters the AWG structure. The measurement over the required spectral range is realized by narrowband tuneable laser source that sends the desired optical signals into the input waveguide through the fiber. After the light travelled through the AWG the broadband optical power meter, connected via fiber to one of the output waveguides, measures the output optical power. The measurement is performed for each output waveguide (channel) in the whole spectral range.

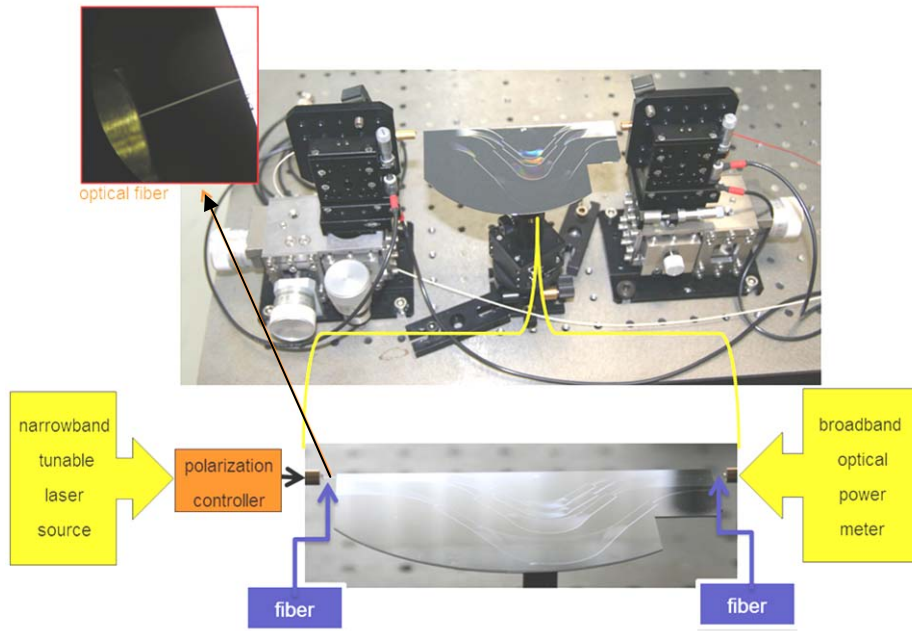


Fig. 6: AWG measurement set-up at ILC Bratislava.

## 7. AWG Design verification

The measured transmission characteristics can be also evaluated using AWG-Analyzer tool. Anyway, the calculation of transmission parameters is usually included in the commercial measurement software tools used by the foundries to measure final chips. Figure 7 shows the measured and simulated transmission characteristics of our designed AWG. As can be seen the characteristics are very similar to each other only the Apollo transmission characteristics feature much lower background crosstalk ( $BX$ ). This is also confirmed by the calculated transmission parameters presented in Table 1 (for more information see [5]). However, simulated and measured transmission parameters reached their theoretical values.

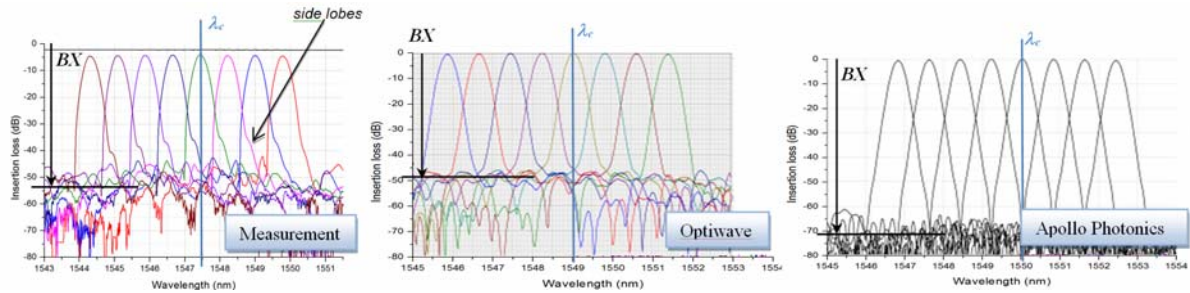


Fig. 7: Measured and simulated AWG transmission characteristics.

Tab. 1. Calculated AWG transmission parameters.

Transmission parameters	AWG-Parameters	Measurement	Optiwave	Apollo
AWG central wavelength	1550.12 nm	1547.50 nm	1549.00 nm	1550.12 nm
Insertion loss	-	6.438 dB	2.624 dB	2.306 dB
Insertion loss uniformity (ILu)	0.7 dB	0.694 dB	0.520 dB	0.760 dB
Adjacent channel crosstalk (AX)	-30 dB	-32.476 dB	-42.024 dB	-50.426 dB
Background crosstalk (BX)	-54.793 dB	-49.458 dB	-71.05 dB	-73.309 dB

## 8. AWG packaging and product promotion

After the transmission parameters (calculated from the AWG measured transmission characteristics) reached required values the AWG chip can be packaged (see Fig. 8-left) and tested under the defined set of temperature and environmental conditions. Only such packaged chips can be used in the real optical networks. Each AWG will be delivered with the datasheet including the most important information about the product (Fig. 8-middle). Product promotion is a final step in the chip production line (Fig. 8-right) [6].

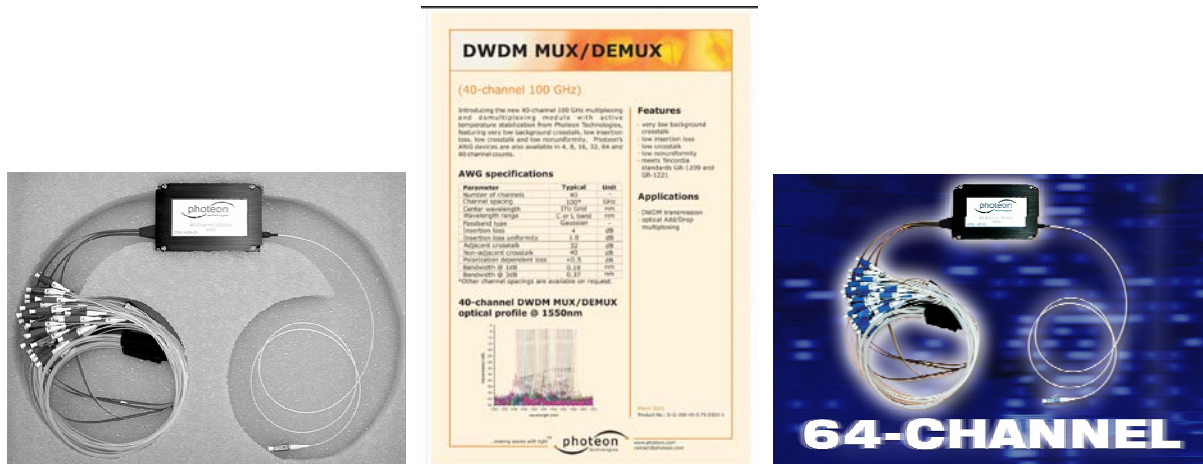


Fig. 8: Packaged AWG chip (left), datasheet (middle) and product promotion (right) [6].

## References:

- [1] K. Okamoto: Fundamentals of Optical Waveguides, Academic Press (2000).
- [2] M.K. Smit, et al.: *J. Select. Topic Quantum Electron.*, **2**, p. 236 (1996).
- [3] D. Seyringer and M. Bielik: In: *SPIE Photonics West 2013*, February 2-7, San Francisco (2013).
- [4] D. Seyringer and P. Schmid: In: *SPIE OSD 2011*, September 5-8, Marseille, France, **8167**, p. 8167 (2011).
- [5] D. Seyringer, F. Uhrek, J. Chovan and A. Kuzma: *ASDAM 2012*, November 11-15, 2012, Smolenice (Slovakia), Published in *IEEE Electron Devices* (2013).
- [6] www.photeon.com.